Matter-wave solitons and finite-amplitude Bloch waves in optical lattices with spatially modulated nonlinearity

Jie-Fang Zhang,[1] Yi-Shen Li,[2] Jianping Meng,[1] Lei Wu,[1] and Boris A. Malomed[3]

[1]*Institute of Nonlinear Physics, Zhejiang Normal University, Jinhua, Zhejiang 321004, P.R. China*
[2]*Department of Mathematics, University of Science and Technology of China, Hefei, Anhui 230026, P.R. China*
[3]*Department of Physical Electronics, Faculty of Engineering, Tel Aviv University, Tel Aviv 69978, Israel*

We investigate solitons and nonlinear Bloch waves in Bose-Einstein condensates trapped in optical lattices (OLs). By introducing specially designed localized profiles of the spatial modulation of the attractive nonlinearity, we construct an infinite set of exact soliton solutions in terms of Mathieu and elliptic functions, with the chemical potential belonging to the semi-infinite gap of the OL-induced spectrum. Starting from the particular exact solutions, we employ the relaxation method to construct generic families of soliton solutions in a numerical form. The stability of the solitons is investigated through the computation of the eigenvalues for small perturbations, and also by direct simulations. Finally, we demonstrate a virtually exact (in the numerical sense) composition relation between nonlinear Bloch waves and solitons.

PACS number(s): 03.75.Lm, 02.30.Jr, 05.30.Jp, 42.65.Tg

I. INTRODUCTION

Analogies between the electron dynamics in perfect crystals and light propagation in periodic optical media suggest a variety of physical phenomena and related applications. Bose-Einstein condensates (BECs) in optical lattices (OLs) not only represent an ideal tool for investigating fundamental effects, such as the Landau-Zener tunneling, Josephson oscillations, dynamical instabilities, and quantum phase transitions between the superfluidity and the Mott insulator, but also offer versatile settings for the potential implementation of quantum computation schemes [1,2].

The mean-field description of the BEC dynamics at zero temperature is based on the Gross-Pitaevskii equation (GPE), that is, the nonlinear Schrödinger equation (NLSE) with a potential term, which is a ubiquitous model with important realizations in other fields—first of all, in nonlinear optics [3]. Many experimental and theoretical works [4–16] (see also reviews [1,2,17,18]) have been dealing with matter-wave and optical solitons in OLs. Usually, these solitons are found in a numerical form, with their chemical potential falling into the semi-infinite gap or finite band gaps of the spectrum induced by the OL potential, in the framework of the corresponding linear Schrödinger equation. A specific issue, which is relevant to the present work, is the composition relation between nonlinear Bloch waves (NBWs) and fundamental solitons, whose main peaks are confined to a single OL cell [19].

Current experiments with BECs wield a high degree of control over key parameters of the systems. By means of the technique of the Feshbach resonance driven by magnetic or optical fields [20,21], one can adjust almost at will the strength and sign of the inter-atomic interactions. On the other hand, available fabrication technologies allow a modulation of the local nonlinearity in nonlinear optics. Therefore, there has been increased interest in the study of the nonlinear dynamics under spatially modulated nonlinearities, in optics and BEC alike, see original works [22–35] and book [36]. In such settings, the nonlinear dynamics exhibits novel features, such as the "anti-Vakhitov-Kolokolov" criterion which controls the stability of gap solitons in media combining a spatially periodic nonlinearity and the OL potential [30].

Exact solutions for matter-wave solitons in BECs with OL potentials are important not only because of their simplicity and the connection to physical bound states, but also since they can be used to test various approximate methods and may also find applications in other fields. The objective of the present work is to construct one-dimensional (1D) soliton solutions in physically relevant situations combining the OL potential and a spatially modulated attractive nonlinearity. In addition to producing exact soliton solutions in specially devised versions of such systems and exhibiting their relation to NBWs, we also find generic numerical solutions, by means the relaxation method, and investigate their stability. The results may be also be directly applied to nonlinear optical media with embedded periodic gratings, which play essentially the same role in photonics as the OLs in BEC.

II. THE MODEL AND ITS REDUCTION

We consider a condensate of atoms trapped by a combination of a tight cigar-shaped magnetic trap and an OL potential acting in the longitudinal direction. If the transverse dimensions are comparable to the healing length, and the longitudinal dimension is much longer than the transverse ones, the setting is effectively one dimensional, obeying by the respective version of the GPE (see, e.g., Refs. [8])

$$i\psi_t = -\psi_{xx} + [2V_0\cos(2x) + g(x)|\psi|^2]\psi, \qquad (1)$$

where $\psi(x,t)$ is the macroscopic wave function of the condensate. Here, time t, spatial coordinates x, and the strength of the OL potential, V_0, are normalized, respectively, by $\hbar/E_r$, k, and $E_r/4$, with the recoil energy $E_r = \hbar^2 k^2/2m$, wave number of the optical lattice k, and atomic mass m. The nonlinearity coefficient is $g = 4m\omega_r a_s/\hbar k^2$, where ω_r is the transverse harmonic frequency and a_s is the s-wave scattering length of inter-atomic collisions. By means of the Feshbach-resonance technique controlled by properly designed configurations of external fields, a_s may be subject

to a spatial modulation, hence the corresponding nonlinearity coefficient $g(x)$ may be a function of x. In this paper, we focus on the attractive nonlinearity, namely, $g(x) < 0$, rather than more general situations with the sign-changing $g(x)$, such as those considered in some other works (see, in particular, Refs. [29,30,35]). It is relevant to mention that the cubic nonlinearity in Eq. (1) is valid if the density is small enough; otherwise, the reduction of the dimension in the GPE from 3 to 1 leads to a nonpolynomial nonlinearity [37].

Stationary soliton solutions to Eq. (1) are searched as $\psi(t,x) = \phi(x) \exp(-i\mu t)$, where chemical potential μ is normalized by the recoil energy, and real function $\phi(x)$ obeys the stationary NLSE,

$$\mu\phi = -\phi_{xx} + [2V_0 \cos(2x) + g(x)\phi^2]\phi, \qquad (2)$$

with boundary conditions $\phi(x \to \pm\infty) = 0$. Up to the rescaling, the number of atoms and energy of the localized state are

$$N = \int_{-\infty}^{\infty} \phi^2 \, dx, \qquad (3)$$

$$\mathcal{E} = \int_{-\infty}^{\infty} \left[\left(\frac{\partial\phi}{\partial x}\right)^2 + 2V_0 \cos(2x)\phi^2 + \frac{g(x)}{2}\phi^4 \right] dx$$

$$\equiv \mu N - \frac{1}{2} \int_{-\infty}^{\infty} g(x)\phi^4 dx. \qquad (4)$$

Following the scheme proposed in Refs. [26,27], *exact* soliton solutions can be constructed by casting Eq. (2) into the form of a *solvable* stationary NLSE in the free space,

$$EU = -U_{XX} + g_0 U^3, \qquad (5)$$

where E and g_0 are constants. This reduction may be implemented by employing the following transformation:

$$\phi(x) = \rho(x)U[X(x)], \quad X(x) \equiv \int_0^x \rho(s)^{-2} ds, \qquad (6)$$

and requiring

$$g(x) = g_0 \rho^{-6}(x), \qquad (7)$$

where ρ obeys the Ermakov-Pinney equation [26–28,38],

$$\rho_{xx} + [\mu - 2V_0 \cos(2x)]\rho = E\rho^{-3}. \qquad (8)$$

It is commonly known that Eq. (5) possesses exact solutions in terms of Jacobi's elliptic functions. Therefore, exact soliton solutions to Eq. (2) can be constructed as long as exact solutions of Eq. (8) are known. In fact,

$$\rho = \sqrt{\alpha\varphi_1^2 + 2\beta\varphi_1\varphi_2 + \gamma\varphi_2^2} \qquad (9)$$

solves the Ermakov-Pinney equation, where α, β, and γ are real constants satisfying $E = (\alpha\gamma - \beta^2)$, and $\varphi_1 = C(\mu,V_0,x)$ and $\varphi_2 = S(\mu,V_0,x)$ are two linearly independent Mathieu functions (cosine and sine, respectively) that satisfy the Mathieu equation [39,40] $\varphi_{xx} + [\mu - 2V_0 \cos(2x)]\varphi = 0$. We here use the notation for solutions to the Mathieu equation adopted in the MAPLE software package. The solutions are defined by the following initial conditions: $C(\mu,V_0,x = 0) = 1$, $\frac{d}{dx}C(\mu,V_0,x)|_{x=0} = 0$, and $S(\mu,V_0,x =$

$0) = 0$, $\frac{d}{dx}S(\mu,V_0,x)|_{x=0} = 1$. In the general case, these solutions are quasiperiodic, therefore they cannot be expressed in terms of the standard set of particular periodic Mathieu functions, ce_n and se_n, nor through the conjugate nonperiodic solutions, fe_n and ge_n [39].

For the soliton solutions to be physical, from Eq. (7) it follows that $\rho(x)$ must not change its sign at any point (a sign-definite function), otherwise the local nonlinearity would diverge at points of $\rho = 0$. Therefore, parameters α, β, γ in Eq. (9) should be chosen so as to secure this condition.

III. EXACT SOLITON SOLUTIONS WITH THE ATTRACTIVE NONLINEARITY

For the attractive nonlinearity, $g_0 < 0$, a relevant exact solution to Eq. (5) is

$$U(X) = \sqrt{(E - \lambda^2)/g_0} \, \text{cn}(\lambda X - X_0, q), \qquad (10)$$

where λ and X_0 are arbitrary constants, E satisfies $-\lambda^2 \leqslant E < \lambda^2$, and cn is the Jacobi's elliptic function with modulus $q = \sqrt{(\lambda^2 - E)/2\lambda^2}$. When $|E| < \lambda^2$, Eq. (10) gives a periodic function of X, with period $4K(q)/|\lambda|$, where $K(q)$ is the complete elliptic integral of the first kind. With regard to $\rho(x) \neq 0$, the boundary condition $\phi(x \to \pm\infty) = 0$ is satisfied when $U(X(x \to \pm\infty)) = 0$. The periodicity of function cn imposes condition $\lambda[X(x \to +\infty) - X(x \to -\infty)] = 2nK(q)$, with integer n. When $E = -\lambda^2$, solution (10) goes over into the well-known elementary one, $U(X) = \sqrt{2E/g_0} \, \text{sech}(\sqrt{-E}X - X_0)$, where the boundary condition $\phi(x \to \pm\infty) = 0$ may be satisfied if $X(x \to \pm\infty) = \infty$.

A. Case of $E = 0$

For $E = 0$, Eq. (8) is linear, and its solution can be a linear combination of the above-mentioned Mathieu functions,

$$\rho = c_1 C(\mu,V_0,x) + c_2 S(\mu,V_0,x), \qquad (11)$$

where constants c_1 and c_2 should be chosen so as to make $\rho(x)$ sign-definite. We begin by constructing exact symmetric and antisymmetric soliton solutions for Eq. (2), where the spatial modulation of the nonlinearity should be represented by an even function $\rho(x)$. Without the loss of generality, we then set $c_1 = 1$ and $c_2 = 0$ in Eq. (11), hence ρ is an even function of x. Since $\rho(x)$ should be a sign-definite function, chemical potential μ cannot be arbitrary for fixed strength V_0 of the OL potential. It can then be shown that, for given V_0, there is a cutoff value of the chemical potential μ_{co}, below which ρ is sign-definite,

$$\mu_{co} \equiv A(0,V_0), \qquad (12)$$

which is exactly the minimum energy eigenvalue in the first Bloch band of the corresponding linear Schrödinger equation with periodic potential $2V_0 \cos(2x)$. Thus, exact soliton solutions of Eq. (2) exist in the semi-infinite gap. The cutoff chemical potential is shown in Fig. 1, where the case $V_0 < 0$ is not shown because μ_{co} is an even function of V_0.
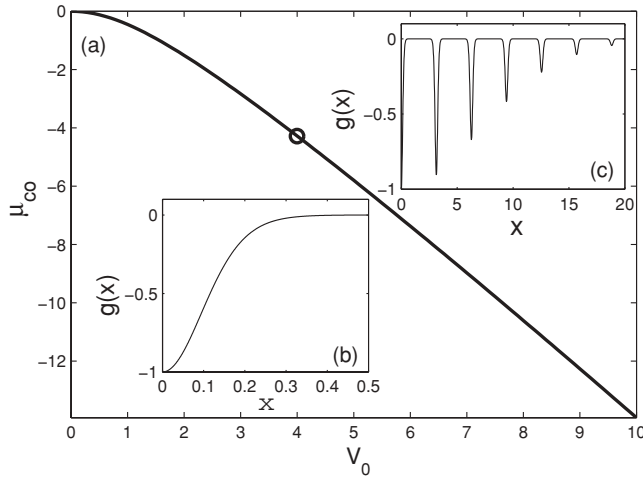
FIG. 1. (a) Cutoff chemical potential, as given by Eq. (12), vs the strength of the OL potential (solid line). Exact soliton solutions exist below the solid line. The circle designates $\mu_{co} = -4.2805$ at $V_0 = 4$. (b) Spatially modulated nonlinearity coefficient, as given by Eq. (13), with $\mu = -10$, $V_0 = 4$, and $g_0 = -1$. (c) Same as in (b), except for $\mu = -4.2807$.

Now we investigate the properties of the nonlinearity-modulation pattern and respective solitons. When μ is much smaller than the cutoff value μ_{co}, $\rho(x)$ increases monotonically and quickly approaches infinity. Therefore, the modulation function

$$g(x) = \frac{g_0}{[C(\mu, V_0, x)]^6} \quad (13)$$

is localized in a very narrow single region [Fig. 1(b)]. Also, from Eqs. (7) and (8) it follows that the smaller the chemical potential, the narrower the localization region. On the contrary, when μ approaches μ_{co}, ρ oscillates and slowly approaches infinity, so that the region of the localization of $g(x)$ is relatively wide, featuring several layers [Fig. 1(c)], and the more closely the chemical potential approaches the cutoff value, the wider the localization region of the nonlinearity coefficient.

Since the even and sign-definite $\rho(x)$ approaches infinity at $|x| \to \infty$, it is clear that $X(x)$, defined in Eq. (6), is a monotonic nondecreasing odd function of x, which has upper and lower limits. Therefore, to let the exact soliton solutions meet the boundary condition $\phi(x \to \pm\infty) = 0$, constant λ in Eq. (10) must be chosen so as to satisfy condition $\lambda X(x \to +\infty) = nK(\sqrt{2}/2)$, where $n = 1, 2, 3, \ldots$. At the same time, constant X_0 should be chosen as $X_0 = 0$ for odd integer n, and $X_0 = K(\sqrt{2}/2)$ for even integer n. Thus, exact soliton solutions to Eq. (2), with the modulation pattern taken as per Eq. (13), are

$$\phi_n(x) = \frac{nK(1/\sqrt{2})}{\sqrt{-g_0}X(+\infty)} C(\mu, V_0, x)$$
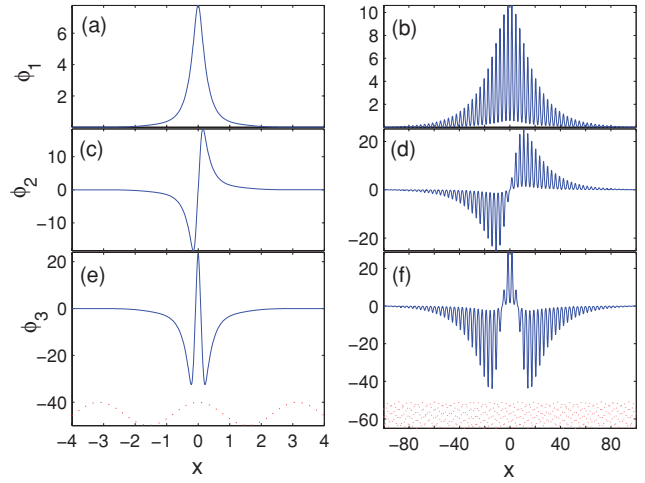$$\times \operatorname{cn}\left(\frac{nK(1/\sqrt{2})}{X(+\infty)}X, \frac{\sqrt{2}}{2}\right), \quad (14)$$

FIG. 2. (Color online) Exact symmetric solitons for (a) $n = 1$ and (e) $n = 3$, and an exact antisymmetric soliton for (c) $n = 2$, where the corresponding modulation function $g(x)$ is taken as per Fig. 1(b) (i.e., with $V_0 = 4$ and $g_0 = -1$). Panels (b), (d), and (f) are the same as (a), (c), and (e), respectively, except for the corresponding modulation function, which is taken as in Fig. 1(c). Solid circles in the bottom of each column show the OL potential.

for $n = 1, 3, 5, \ldots$, while for $n = 2, 4, 6, \ldots$, the exact solutions are

$$\phi_n(x) = \frac{nK(1/\sqrt{2})}{\sqrt{-g_0}X(+\infty)} C(\mu, V_0, x)$$
$$\times \operatorname{cn}\left[\frac{nK(1/\sqrt{2})}{X(+\infty)}X - K\left(\frac{\sqrt{2}}{2}\right), \frac{\sqrt{2}}{2}\right], \quad (15)$$

where we define $X(x) = \int_0^x C(\mu, V_0, s)^{-2} ds$.

It follows from Eqs. (6), (13)–(15) that, once the chemical potential ($\mu < \mu_{co}$), constant g_0, and the strength of the OL potential, V_0, are fixed, there exists an *infinite number* of exact solitons sharing the same chemical potential. Note that expression (14) is an even function of x, hence the soliton is symmetric. On the contrary, expression (15) is an odd function of x, which varies $\sim x$ at $x \to 0$, yielding an antisymmetric soliton. In either case, the matter-wave densities are even functions of x. The exact soliton solution, ϕ_n, possesses $n - 1$ density nodes (see Figs. 2 and 3), and from Eq. (4) it can be concluded that the larger the n, the larger the energy of the corresponding BEC state. Thus one may conclude that ϕ_1 corresponds to the ground state, ϕ_n corresponding to the $(n - 1)$th excited states. By comparing the exact soliton solution ϕ_1 to the ground-state solution of the same GPE, obtained in a numerical form by means of the imaginary-time method, we find that ϕ_1 is identical to the ground state when $V_0 < 0$. However, ϕ_1 is not always the ground state when $V_0 > 0$ (for instance, ϕ_1 remains the ground-state solution at $\mu < -9$ for $V_0 = 4$). On the other hand, for the 1D linear Schrödinger equation, it is well known that localized states with different energy eigenvalues are orthogonal. Here we find that the localized states of the *nonlinear* GPE are *not* orthogonal.

From Figs. 1 and 2 it can be found that the widths of solitons are proportional to the widths of the respective
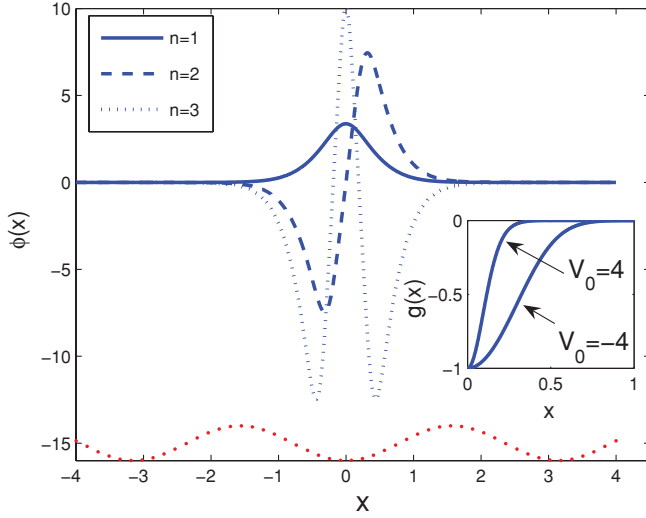
FIG. 3. (Color online) Exact symmetric and antisymmetric solitons with chemical potential $\mu = -10$. The parameters are $V_0 = -4$, $g_0 = -1$. Solid circles show the OL potential.
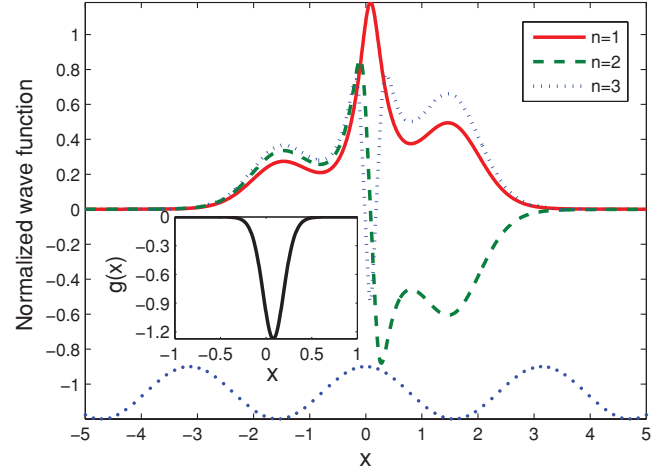

FIG. 4. (Color online) Normalized exact asymmetric solitons, $\phi_n N_n^{-1/2}$, where N_n is the respective norm (scaled number of atoms). Inset: the corresponding asymmetric nonlinearity-modulation profile. Here, we set $g_0 = -1$, with other parameters given in the text. Solid circles show the OL potential.

nonlinearity-modulation profiles $g(x)$. This is understandable because both the widths of the solitons and $g(x)$ profiles are determined by $\rho(x)$, see Eqs. (6) and (7). That is, the more rapidly $\rho(x)$ approaches infinity, the narrower the solitons and $g(x)$ distributions are. Further, it can be shown that the widths of the exact solitons are always larger than those of the respective modulation profiles. To analyze this point in a simple form, we here take the case of $V_0 = 0$. In this case, $\mu < \mu_{\text{co}} = 0$, $\rho \sim \exp(\sqrt{-\mu}x)$, so that $g \sim \exp(-6\sqrt{-\mu}x)$ and $X \sim 1 - \exp(-2\sqrt{-\mu}x)$ at $x > 0$; thus the width of the soliton is about three times larger than that of the $\rho(x)$ modulation. Since exact solitons in the left column of Fig. 2 are confined mainly to a single OL cell, they may be called fundamental solitons [19], whereas the right column displays broader modes similar to the *gap waves* reported in Refs. [41].

Another noteworthy point is that, although the cutoff chemical potential μ_{co} is an even function of V_0, the nonlinearity-modulation function is not. From Eqs. (8) and (13), it follows that the width of $g(x)$ corresponding to $V_0 > 0$ is smaller than that for $-V_0$ when the chemical potential is fixed; see a typical example of the comparison in the inset to Fig. 3. Thus, the effective nonlinearity in the case of $-V_0 < 0$ is stronger than for $V_0 > 0$, at the same g_0. On the other hand, the effective potential is attractive (repulsive) for negative (positive) V_0 for fundamental solitons. For these reasons, the number of atoms in the exact fundamental solitons with $V_0 < 0$ is smaller than for $V_0 > 0$, as can be seen from the comparison of Figs. 2 and 3.

Similarly, exact asymmetric solitons to Eq. (2) can be constructed if we let $c_1 c_2 \neq 0$ in Eq. (11). For ρ to be sign-definite in this case, we again need $\mu < \mu_{\text{co}}$, and c_1, c_2 should be chosen properly. As a generic example, we take $\mu = -5$, $V_0 = 4$, and $c_2 = g_0 = -c_1 = -1$. In such a case, $\rho(x) = C(-5, 4, x) - S(-5, 4, x)$, the asymmetric modulation profile of $g(x)$ is given by Eq. (7), and $X(x) = \int_0^x \rho^{-2}(s)\,ds$. To meet the boundary conditions $\phi(x \to \pm\infty) = 0$, constants

λ and X_0 in Eq. (10) should satisfy

$$
\begin{aligned}
\lambda[X(+\infty) - X(-\infty)] &= 2nK(\sqrt{2}/2), \\
X_0 &= \lambda X(-\infty) + K(\sqrt{2}/2),
\end{aligned}
\tag{16}
$$

where $n = 1, 2, 3, \ldots$.

Exact asymmetric solitons can be found when substituting values (16) into Eqs. (6) and (10). The representative profiles of the solitons, together with the corresponding asymmetric nonlinearity-modulation profile, are displayed in Fig. 4. Similar to the exact symmetric and antisymmetric solutions, different solitons with the same chemical potential are not orthogonal.

B. Case of $E > 0$

The exact solution to Eq. (5) with $E > 0$ is given by Eq. (10). To construct exact localized solutions, $\rho(x)$ should approach infinity as $|x| \to \infty$, so that the function $X(x)$ is bounded; it can be shown that such a requirement may be realized when chemical potential μ falls into the band gaps of the spectrum induced by the OL potential of the corresponding linear Schrödinger equation. The exact solution for ρ is given by Eq. (9). Due to the nonzero value of the corresponding Wronskian, $\varphi_1'\varphi_2 - \varphi_1\varphi_2' = -1$, $\varphi_1(x)$ and $\varphi_2(x)$ cannot vanish at the same position, and ρ is always sign-definite. However, if μ does not belong to the semi-infinite gap, there exist several points where ρ is very close to zero, making the strength of the nonlinearity very large [this region is very narrow, and $g(x)$ looks like the δ function], which we do not consider here. We are rather interested in the case of $\mu < \mu_{\text{co}}$.

To meet the boundary condition, we need $\lambda[X(\infty) - X(-\infty)] = 2nK(q)$, $n = 1, 2, 3, \ldots$. Because $\lambda > \sqrt{E}$, an inequality ensues from here,

$$
nK\left(\frac{\lambda^2 - E}{2\lambda^2}\right) > \frac{X(\infty) - X(-\infty)}{2}\sqrt{E}.
\tag{17}
$$

From Eq. (17) it follows that $n > n_{max} \equiv [X(\infty) - X(-\infty)]\sqrt{E}/\pi$. Thus, unlike the case of $E = 0$, where all values $n = 1,2,3,\ldots$ give rise to solitons, here the first several values of n may disappear. For example, if $n_{max} = 2.5$, then actual values which give rise to the solitons are $n = 3,4,5,\ldots$. However, in the semi-infinite gap, we find $n_{max} < 1$, regardless of values of E, α, β, and γ. That is to say, there is still an *infinite number* of exact solitons sharing the same chemical potential. The exact soliton solutions are given by Eqs. (6), (9), and (10), with the nonlinearity given by Eq. (7).

C. Case of $E < 0$

In this case, the sign-definite ρ exists when the chemical potential is in the semi-infinite gap, that is, $\mu < \mu_{co}$, and the real constants α, β, and γ should be carefully chosen. To meet the boundary condition, we need $\lambda[X(\infty) - X(-\infty)] = 2nK(q)$, $n = 1,2,3,\ldots$. Unlike the case of $E > 0$, where inequality (17) must be satisfied, here there is no restriction on n, hence there still exists an infinite number of exact solitons sharing the same chemical potential.

D. Discussion

Thus far, we have demonstrated that an infinite number of exact soliton solutions, which share common values of the chemical potential, can be constructed in the model with the OL potential. These solutions exist in the semi-infinite gap, in accordance with the fact that soliton families [n in Eqs. (14) and (15) denotes the family's index] can be found in the semi-infinite gap when the attractive nonlinearity is spatially uniform [19,42]. The same model also supports gap solitons in finite band gaps; we are not going to discuss exact solitons in those band gaps because (i) the exact spatially modulated nonlinearity mimics an array of δ functions, which may be hard to realize in experiments, and (ii) the corresponding profile of exact solitons are irregular.

We did not analyze in detail properties of exact solitons when $E \neq 0$, because they are similar to what was described above for $E = 0$. For example, when $E \neq 0$, exact symmetric and antisymmetric solutions can be constructed by choosing $\beta = 0$ and $\beta \neq 0$, respectively, in Eq. (9).

We did not consider the repulsive nonlinearity either. The reason is that for repulsive nonlinearities ($g_0 > 0$), a nontrivial solution to Eq. (5) is $U(x) = \sqrt{2(E - \lambda^2)/g_0} \, \text{sn}(\lambda X - X_0, \sqrt{E/\lambda^2 - 1})$, where $\lambda^2 < E < 2\lambda^2$. To meet the boundary condition in this case, we must demand $\lambda[X(\infty) - X(-\infty)] = 2nK(\sqrt{E/\lambda^2 - 1})$, $n = 1,2,3,\ldots$, from which it follows that $n < n_{max} \equiv [X(\infty) - X(-\infty)]\sqrt{E}/\pi$. On the other hand, we have $n_{max} < 1$ for the chemical potential falling into the semi-infinite gap. Therefore, there are no exact solitons in the semi-infinite gap for the spatially modulated repulsive nonlinearity, just as in the case of the spatially uniform repulsive nonlinearity [1].

IV. NUMERICALLY FOUND SOLITONS AND THEIR STABILITY

In Sec. III, we were able to find only discrete sets of particular exact soliton solutions for the given nonlinearity.

Here we consider more general matter-wave solitons with different values of the chemical potential in the OL potential, when the localized nonlinearity-modulation profile is fixed. That is, we aim to find solitons in the framework of the equation

$$\mu\phi = -\phi_{xx} + 2V_0\cos(2x)\phi - [C(\mu_0,V_0,x)]^{-6}\phi^3, \quad (18)$$

with $\mu_0 < \mu_{co}$ and, generally speaking, $\mu \neq \mu_0$, where μ_{co} is given by Eq. (12). We focus here only on symmetric soliton solutions in the semi-infinite gap, that is, at $\mu < \mu_{co}$.

Exact solutions to Eq. (18) have been found above for $\mu = \mu_0$. Using these exact solutions as an an initial guess, one can find more general solitons by means of the numerical relaxation method. There are two different cases, which we define as I and II, with $g(x)$ localized, respectively, around a peak or bottom of the OL potential, for positive or negative V_0, respectively. In either case, solitons can be found in the semi-infinite gap, regardless of the value of μ_0. In case II, the number of atoms is a monotonously decreasing function of μ, just like in the case of the NLSE with the spatially uniform attractive nonlinearity. However, the situation is quite different in case I. For the first family of solitons ($n = 1$), we find that the number of atoms at first decreases and then increases with the increase of μ, see Fig. 5(b), whereas for other soliton families, the atom number is a monotonously increasing function of μ, see Fig. 5(d). These types of the dependences have obvious implications for soliton stability, as per the Vakhitov-Kolokolov criterion [43], see below. For all soliton families in case I, when μ approaches the cutoff value, most atoms are located in wells of the OL potential adjacent to the region where the nonlinearity is concentrated. In other
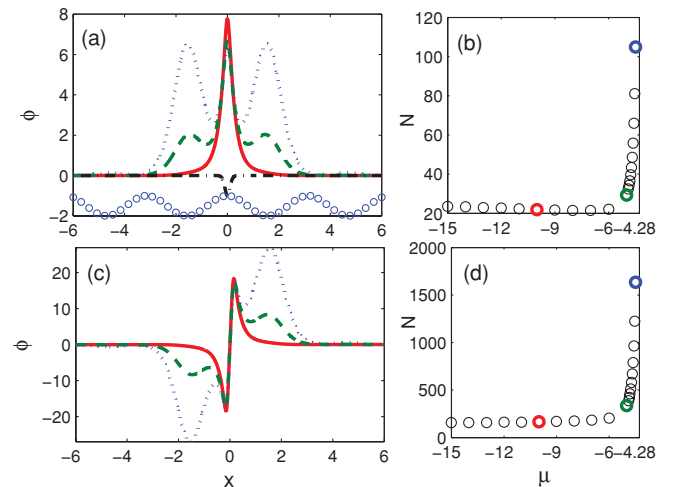

FIG. 5. (Color online) (a) First family of numerically found solitons. Solid (red), dashed (green), and dotted (blue) lines represent the solitons with chemical potentials $\mu = -10$, $\mu = -5$, and $\mu = -4.5$, respectively. The dashed-dotted line shows the nonlinearity-modulation profile, with $\mu_0 = -10$ and $V_0 = 4$, see Eq. (18) (this corresponds to what is defined as case I in the text). Chains of open circles show the OL potential. (b) The number of atoms vs the chemical potential. Panels (c) and (d): The same as (a) and (b), except that the solitons are from the second family.
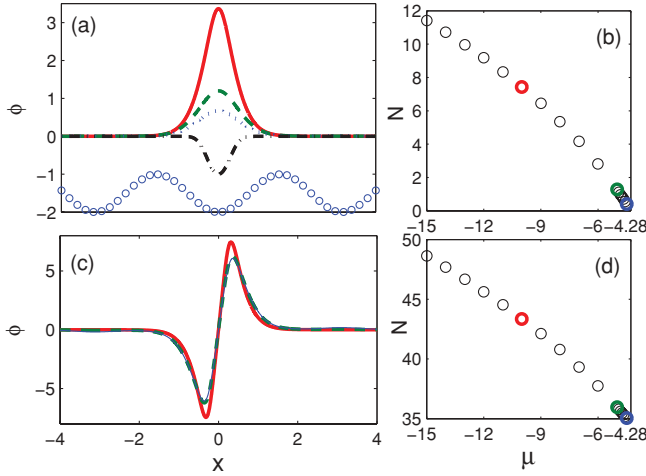
FIG. 6. (Color online) Same as Fig. 5, except for $V_0 = -4$ (which corresponds to case II, as defined in the text). Note that in (c), the solitons of $\mu = -5$ and $\mu = -4.5$ are almost indistinguishable.

FIG. 8. (Color online) Example of the evolution of an unstable soliton. The nonlinearity-modulation function and OL potential are the same as in Fig. 5(a). The initial condition is taken as per the numerically calculated solution [the dashed (green) line in Fig. 5(a)], mixed with a random (white-noise) perturbation.

words, the solitons are confined to one or two OL cells in case I, while in case II they are trapped in a single cell (see Fig. 6).

To investigate the stability of solitons, we first employ the linear-stability analysis. Substituting a perturbed solution, $\psi(x,t) = [\phi(x) + u(x) \exp(i\Delta t) + v^*(x) \exp(-i\Delta^* t)] \exp(-i\mu t)$, into Eq. (1) and linearizing it around the unperturbed one, $\phi(x)$, we arrive at an eigenvalue problem,

$$\begin{pmatrix} \mathcal{L} & -g\phi^2 \\ g\phi^2 & -\mathcal{L} \end{pmatrix} \begin{pmatrix} u \\ v \end{pmatrix} = \Delta \begin{pmatrix} u \\ v \end{pmatrix}, \tag{19}$$

with operator $\mathcal{L} = d^2/dx^2 + \mu - 2V_0 \cos(2x) - 2g\phi^2$, and $g = -[C(\mu_0, V_0, x)]^{-6}$. The soliton is unstable if any eigenvalue Δ has an imaginary part.

Results of numerical calculations, displayed in Fig. 7 (the largest instability growth rate δ is the maximum absolute value of the imaginary part of Δ), reveal that, in case II, the first and second families of solitons are *stable* against small perturbations, while higher-order soliton families are unstable. On the other hand, for case I, stable solitons emerge only in the first family, when the chemical potential is small enough, so that the solitons are very narrow, and the nonlinearity is strong enough to sustain solitons in the presence of the locally repulsive OL potential. Similar conclusions concerning the stability of solitons supported by the competing (locally
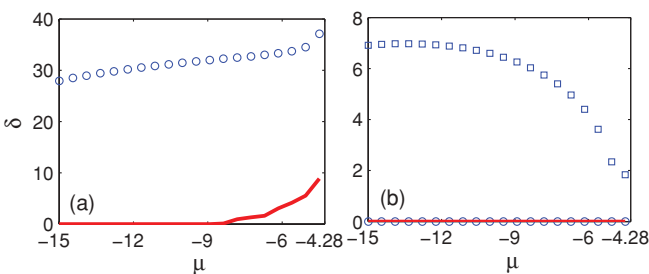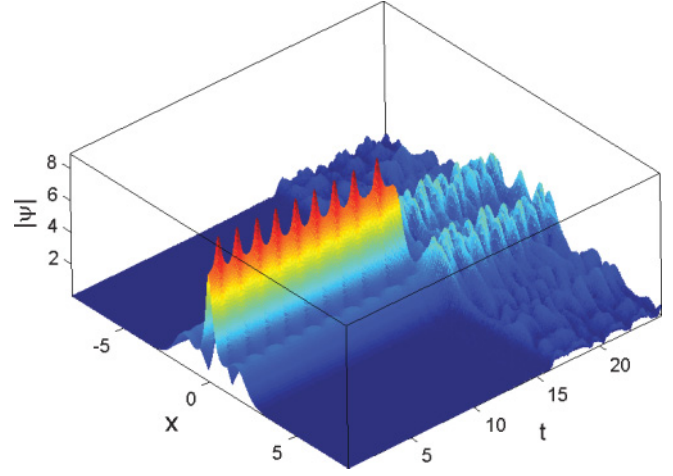

FIG. 7. (Color online) Largest instability growth rate δ vs the chemical potential. Solid lines, circles, and squares pertain to the first, second, and third families of the solitons, respectively. The parameters in (a) and (b) are the same as in Figs. 5 and 6, respectively.

attractive or repulsive) linear and nonlinear potentials were reported in Ref. [35]. Comparing the data displayed in Fig. 7 with panels (b) and (d) in Figs. 5 and 6, we conclude that the Vakhitov-Kolokolov criterion ($dN/d\mu < 0$, which is known as the necessary criterion for the stability of solitons supported by the attractive nonlinearity [43]) holds in the present model. We have also checked the stability of exact soliton solutions. The results are in qualitative agreement with those shown in Fig. 7.

The stability of the solitons was further checked by direct numerical simulations of Eq. (1), producing results complying with the predictions of the linear-stability analysis. In particular, the solitons from the first family in the unstable region originally exhibit a quasistable evolution and then decay, with a larger part of the atom number located in a neighboring well of the OL, see Fig. 8, while unstable solitons from other families quickly decay into noise.

Although we have displayed here the results of the stability investigation only for two examples of the nonlinearity-modulation profile, similar conclusions hold for other values of μ_0 and V_0 as well. The asymmetric solitons too demonstrate a similar behavior.

V. COMPOSITION RELATION BETWEEN SOLITONS AND NONLINEAR BLOCH WAVES

Figure 6 suggests that, in many cases, the solitons and corresponding $g(x)$ modulation profiles are confined to a single cell. Then, it may be interesting to form a spatially periodic nonlinearity pattern, by placing the same local profiles of $g(x)$ into other wells of the OL potential. In such a case, the system may admit not only the solitons, but also NBWs. For the NLSE with the spatially uniform nonlinearity, the intuitive concept of the NBWs built as chains of fundamental solitons has been recently justified in Ref. [19], which produced a composition relation between NBWs and fundamental solitons, although the relation cannot be expressed in a simple mathematical form.

In this section, we demonstrate that the composition relation is also numerically valid in the GPE with the spatially periodic nonlinearity. To this end, we consider the following periodic nonlinearity-modulation pattern:

$$g_p(x) = \sum_m g_0 \left[C(\mu_0, V_0, x - m\pi) \right]^{-6}, \tag{20}$$

where $m = 0, \pm 1, \pm 2, \dots$, and the summation is performed over cells of the OL potential.

For many values of μ, the single-peak modulation profile for $g(x)$ given by Eq. (13), and the respective soliton given by Eqs. (14) and (15), are confined to a single OL cell (here we focus on the symmetric case). For instance, $g(x)$ and the soliton solution for $\mu = \mu_0 = -25$ at $V_0 = -4$ meet this condition. In such cases, adjacent solitons practically do not overlap, hence forces of the interaction between them in the periodic configuration are negligible. Therefore, one may try to represent NBWs supported by the modulation pattern (20) as chains of fundamental solitons with identical or alternating signs:

$$(\phi_{\text{NBW}})_1 = \sum_m \phi_n(x - m\pi), \tag{21}$$

$$(\phi_{\text{NBW}})_2 = \sum_m (-1)^m \phi_n(x - m\pi), \tag{22}$$

where ϕ_n is given by Eq. (14) or (15). The NBW corresponding to Eq. (21) is located at the center of the respective Brillouin zone, while the "staggered" one, represented by Eq. (22), is at its edge. The conjectured composition relation between the NBW and fundamental solitons was checked numerically for the first and second soliton families, as shown in Fig. 9. For
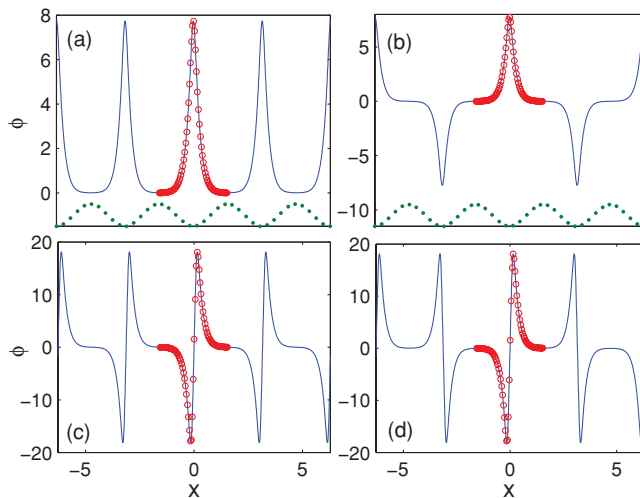
FIG. 9. (Color online) Composition relation between NBWs and fundamental solitons. Chains of open circles in (a) and (b) represent fundamental solitons from the first family, while in (c) and (d) the circles denote fundamental solitons from the second family. Solid lines in (a) and (c) are NBWs found at the center of the Brillouin zone, while in (b) and (d) they depict the NBWs at the edge of the Brillouin zone. Profiles of the numerically computed NBWs completely overlap with the expressions given by Eqs. (21) and (22). The periodic nonlinearity-modulation profile is given by Eq. (20), with $g_0 = -1$, $\mu = \mu_0 = -25$, and $V_0 = -4$. Chains of solid circles show the OL potential.
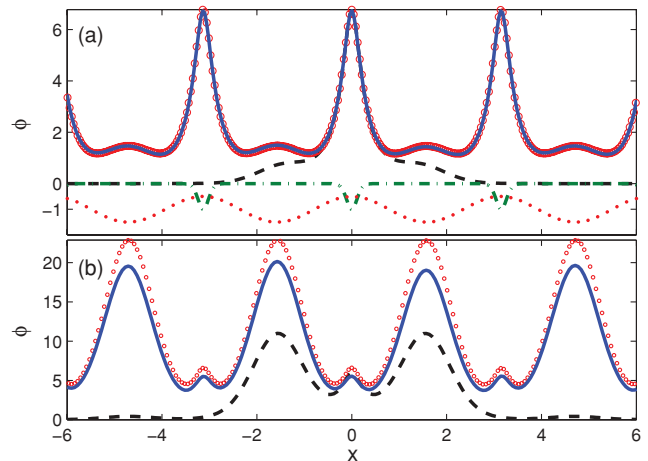
FIG. 10. (Color online) Examples of situations when the composition relation between NBWs and fundamental solitons holds (a) and does not hold (b). Dashed lines: individual fundamental solitons, belonging to the first soliton family, of which the NBWs are built. Solid lines: numerically obtained NBWs at the center of Brillouin zone. Chains of open circles: NBWs given by Eq. (21). The periodic nonlinearity-modulation profile, depicted by the dashed-dotted (green) line in (a), is given by Eq. (20) with $g_0 = -1$, $V_0 = 4$, and $\mu_0 = -6$. The chemical potentials of the solitons and NBWs in (a) and (b) are, respectively, $\mu = -6$ and $\mu = -4.4$.

other families of solitons, the composition relation also holds, in the same sense.

When the soliton's width exceeds the period of the underlying OL, the composition relation between NBWs and fundamental solitons, as given by Eqs. (21) and (22), still holds if the width of the soliton remains smaller than two OL periods; see a typical example in Fig. 10(a). Actually, the composition relation holds because the underlying GPE is almost linear in regions between adjacent solitons. Numerical computations also demonstrate that, in addition to the periodic NBWs, one can build confined extended states as chains of several fundamental solitons, with arbitrary combination of the signs, see Refs. [19,42].

However, the composition method no longer applies as the soliton widths grow too large, see Fig. 10(b). Therefore, the final conclusion is that the numerically tested composite relation remains valid as long as the width of the individual soliton does not exceed two OL periods. On the other hand, if the nonlinearity is spatially uniform (unmodulated), the composite relation is numerically correct provided that the width of the individual soliton does not exceed *one* OL period, as conjectured and verified in another context in Ref. [19]). Thus, the use of the nonlinearity modulation helps to expand the validity of the composition method.

VI. CONCLUSIONS

We have constructed an infinite number of exact soliton solutions, both symmetric and asymmetric, in the model of the BEC with the OL potential and specially devised profiles of the spatial modulation of the local attractive nonlinearity. The chemical potential of the exact solutions falls into the

semi-infinite gap. These solitons may coexist, with different energies, at common values of the chemical potential.

Based on the set of particular exact solutions, we have also found generic soliton families in the numerical form, fixing the nonlinearity-modulation profile. The stability of the numerically found solitons has been checked by means of the linear-stability analysis and by using direct simulations.

Finally, we have discussed the composition relation between nonlinear Bloch waves and the fundamental solitons. We have demonstrated numerically that the composition relation

is virtually exact when widths of the solitons do not exceed the double period of the OL.

[1] O. Morsch and M. Oberthaler, Rev. Mod. Phys. **78**, 179 (2006).

[2] B. A. Malomed, D. Mihalache, F. Wise, and L. Torner, J. Optics B **7**, R53 (2005).

[3] G. Agrawal, *Applications of Nonlinear Fiber Optics*, 2nd ed. (Academic, San Diego, 2001).

[4] B. P. Anderson and M. A. Kasevich, Science **282**, 1686 (1998).

[5] K. Berg-Sørensen and K. Mølmer, Phys. Rev. A **58**, 1480 (1998).

[6] D. I. Choi and Q. Niu, Phys. Rev. Lett. **82**, 2022 (1999).

[7] B. Wu and Q. Niu, Phys. Rev. A **61**, 023402 (2000); **64**, 061603(R) (2001); B. Wu, R. B. Diener, and Q. Niu, *ibid.* **65**, 025601 (2002).

[8] J. C. Bronski, L. D. Carr, B. Deconinck, and J. N. Kutz, Phys. Rev. Lett. **86**, 1402 (2001); J. C. Bronski, L. D. Carr, B. Deconinck, J. N. Kutz, and K. Promislow, Phys. Rev. E **63**, 036612 (2001); J. C. Bronski, L. D. Carr, R. Carretero-González, B. Deconinck, J. N. Kutz, and K. Promislow, *ibid.* **64**, 056615 (2001).

[9] A. Trombettoni and A. Smerzi, Phys. Rev. Lett. **86**, 2353 (2001).

[10] P. J. Y. Louis, E. A. Ostrovskaya, C. M. Savage, and Y. S. Kivshar, Phys. Rev. A **67**, 013602 (2003).

[11] D. N. Neshev, T. J. Alexander, E. A. Ostrovskaya, Y. S. Kivshar, H. Martin, I. Makasyuk, and Z. Chen, Phys. Rev. Lett. **92**, 123903 (2004); Z. Chen, H. Martin, E. D. Eugenieva, J. Xu, and A. Bezryadina, *ibid.* **92**, 143902 (2004).

[12] T. Anker, M. Albiez, R. Gati, S. Hunsmann, B. Eiermann, A. Trombettoni, and M. K. Oberthaler, Phys. Rev. Lett. **94**, 020403 (2005).

[13] G. Theocharis, D. J. Frantzeskakis, R. Carretero-González, P. G. Kevrekidis, and B. A. Malomed, Phys. Rev. E **71**, 017602 (2005).

[14] R. Scharf and A. R. Bishop, Phys. Rev. E **47**, 1375 (1993); B. B. Baizakov, B. A. Malomed, and M. Salerno, Eur. Phys. J. D **38**, 367 (2006).

[15] X. F. Zang, C. Jiang, and H. B. Zhu, Phys. Rev. E **80**, 036604 (2009).

[16] J. Wang, J. Yang, T. J. Alexander, and Y. S. Kivshar, Phys. Rev. A **79**, 043610 (2009).

[17] V. A. Brazhnyi and V. V. Konotop, Mod. Phys. Lett. B **18**, 627 (2004); F. Kh. Abdullaev, A. Cammal, A. M. Kamchatnov, and L. Tomio, Int. J. Mod. Phys. B **19**, 3415 (2005).

[18] *Emergent Nonlinear Phenomena in Bose-Einstein Condensates*, ed. by P. G. Kevrekidis, D. J. Frantzeskakis, and R. Carretero-González (Springer, Berlin, 2008).

[19] Y. Zhang and B. Wu, Phys. Rev. Lett. **102**, 093905 (2009); Y. Zhang, Z. Liang, and B. Wu, Phys. Rev. A **80**, 063815 (2009).

[20] S. Inouye, M. R. Andrews, J. Stenger, H.-J. Miesner, D. M. Stamper-Kurn, and W. Ketterle, Nature (London) **392**, 151 (1998).

[21] M. Theis, G. Thalhammer, K. Winkler, M. Hellwig, G. Ruff, R. Grimm, and J. H. Denschlag, Phys. Rev. Lett. **93**, 123001 (2004).

[22] I. Towers and B. A. Malomed, J. Opt. Soc. Am. **19**, 537 (2002).

[23] F. Kh. Abdullaev, J. G. Caputo, R. A. Kraenkel, and B. A. Malomed, Phys. Rev. A **67**, 013605 (2003); H. Saito and M. Ueda, Phys. Rev. Lett. **90**, 040403 (2003).

[24] G. Theocharis, P. Schmelcher, P. G. Kevrekidis, and D. J. Frantzeskakis, Phys. Rev. A **72**, 033614 (2005).

[25] M. I. Rodas-Verde, H. Michinel, and V. M. Pérez-García, Phys. Rev. Lett. **95**, 153903 (2005).

[26] J. Belmonte-Beitia, V. M. Pérez-García, V. Vekslerchik, and P. J. Torres, Phys. Rev. Lett. **98**, 064102 (2007).

[27] J. Belmonte-Beitia, V. M. Pérez-García, V. Vekslerchik, and V. V. Konotop, Phys. Rev. Lett. **100**, 164102 (2008).

[28] V. M. Pérez-García, P. J. Torres, and G. D. Montesinos, SIAM J. Appl. Math. **67**, 990 (2007).

[29] H. Sakaguchi and B. A. Malomed, Phys. Rev. E **73**, 026601 (2006); Phys. Rev. A **75**, 063825 (2007).

[30] H. Sakaguchi and B. A. Malomed, Phys. Rev. A **81**, 013624 (2010).

[31] F. K. Abdullaev and J. Garnier, Phys. Rev. A **72**, 061605(R) (2005); F. Abdullaev, A. Abdumalikov, and R. Galimzyanov, Phys. Lett. A **367**, 149 (2007); F. K. Abdullaev, A. Gammal, M. Salerno, and L. Tomio, Phys. Rev. A **77**, 023615 (2008); F. K. Abdullaev, R. M. Galimzyanov, M. Brtka, and L. Tomio, Phys. Rev. E **79**, 056220 (2009).

[32] G. Theocharis, P. Schmelcher, P. G. Kevrekidis, and D. J. Frantzeskakis, Phys. Rev. A **72**, 033614 (2005); **74**, 053614 (2006).

[33] Y. Sivan, G. Fibich, and M. I. Weinstein, Phys. Rev. Lett. **97**, 193902 (2006); Y. Sivan, G. Fibich, B. Ilan, and M. I. Weinstein, Phys. Rev. E **78**, 046602 (2008); Y. V. Kartashov, V. A. Vysloukh, and L. Torner, Opt. Lett. **33**, 1747 (2008); **33**, 2173 (2008); Y. V. Kartashov, B. A. Malomed, V. A. Vysloukh, and L. Torner, *ibid.* **34**, 770 (2009); C. Hang, V. V. Konotop, and G. Huang, Phys. Rev. A **79**, 033826 (2009).

[34] Y. V. Kartashov, V. A. Vysloukh, and L. Torner, Opt. Lett. **33**, 1747 (2008); Y. V. Kartashov, V. A. Vysloukh, A. Szameit, F. Dreisow, M. Heinrich, S. Nolte, A. Tünnermann, T. Pertsch, and L. Torner, *ibid.* **33**, 1120 (2008); Y. V. Kartashov, B. A. Malomed, V. A. Vysloukh, and L. Torner, *ibid.* **34**, 3625 (2009).

[35] C. H. Tsang, B. Malomed, and K. W. Chow, DCDS-S (to be published).

[36] B. A. Malomed, *Soliton Management in Periodic Systems* (Springer, New York, 2006).

[37] L. Salasnich, A. Parola, and L. Reatto, Phys. Rev. A **65**, 043614 (2002); A. E. Muryshev, G. V. Shlyapnikov, W. Ertmer, K. Sengstock, and M. Lewenstein, Phys. Rev. Lett. **89**, 110401 (2002); A. Muñoz Mateo and V. Delgado, Phys. Rev. A **77**, 013617 (2008).

[38] V. P. Ermakov, Univ. Izv. Kiev **20**, 1 (1880); E. Pinney, Proc. Am. Math. Soc. **1**, 681 (1950).

[39] M. Abramowitz and I. Stegun, *Handbook of Mathematical Functions* (Dover, New York, 1965).

[40] D. Frenkel and R. Portugal, J. Phys. A **34**, 3541 (2001).

[41] T. Anker, M. Albiez, R. Gati, S. Hunsmann, B. Eiermann, A. Trombettoni, and M. K. Oberthaler, Phys. Rev. Lett. **94**, 020403 (2005); T. J. Alexander, E. A. Ostrovskaya, and Y. S. Kivshar, *ibid.* **96**, 040401 (2006).

[42] T. J. Alexander and Y. S. Kivshar, Appl. Phys. B **82**, 203 (2006).

[43] M. G. Vakhitov and A. A. Kolokolov, Sov. J. Radiophys. Quantum Electron. **16**, 783 (1973).